Available online at www.sciencedirect.com
ScienceDirect
Journal of Power Sources 160 (2006) 627–632
JOURNAL OF POWER SOURCES
www.elsevier.com/locate/jpowsour

Electrochemical characteristics of layered $LiNi_{1/3}Co_{1/3}Mn_{1/3}O_2$ and with different synthesis conditions

Ping He [a,*], Haoran Wang [b], Lu Qi [a], Tetsuya Osaka [c]

[a] *Department of Applied Chemistry, College of Chemistry and Molecular Engineering, Peking University, Beijing 100871, PR China*
[b] *Beijing Green Power and Technology Company Ltd., Beijing 100001, PR China*
[c] *Department of Applied Chemistry, Waseda University, 3-4-1 Okubo, Shinjuku-ku, Tokyo 169-8555, Japan*

Received 13 December 2005; received in revised form 17 January 2006; accepted 18 January 2006
Available online 28 February 2006

Abstract

$LiNi_{1/3}Mn_{1/3}Co_{1/3}O_2$ had been successfully prepared from spherical composite carbonate via a simple uniform-phase precipitation method [P. He, H. Wang, L. Qi, T. Osaka, J. Power Sources, in press] at normal pressure, using nickel, cobalt and manganese sulfate and ammonia bicarbonate as reactants. The preparation of spherical composite carbonate was significantly dependant on synthetic condition, such as the reaction temperature, feed rate, molar ratio of these reactants, etc. The optimized condition resulted in spherical composite carbonate of which the particle size distribution was uniform, as observed by scanning electronic microscopy (SEM). Calcination of the uniform composite carbonate with lithium carbonate at high temperature led to a well-ordered layer structured $LiNi_{1/3}Mn_{1/3}Co_{1/3}O_2$ as confirmed by X-ray diffraction (XRD), without obvious change in shape. Due to the homogeneity of the composite carbonate, the final product, $LiNi_{1/3}Mn_{1/3}Co_{1/3}O_2$, was also significantly uniform, i.e., the average particle size was of about 10 μm in diameter and the distribution was relatively narrow. As a result, the corresponding tap density was also high, approximately 2.32 g cm^{-3}, of which the value is very near to that of commercialized $LiCoO_2$. In the voltage range of 2.8–4.2, 2.8–4.35 and 2.8–4.5 V, the discharge capacities of $LiNi_{1/3}Mn_{1/3}Co_{1/3}O_2$ electrode were 159, 168 and 179 mAh g^{-1}, respectively, with good cyclability.

Keywords: Spherical; Composite carbonate; Uniform-phase precipitation; Lithium-ion cell; Cathode material

1. Introduction

Currently, the most widely used cathode material in lithium-ion secondary battery is $LiCoO_2$, because of its simple producing process, high specific capacity and long circle life [1]. While concerning about the relatively high cost of cobalt, its safety when abused and the interesting higher specific capacity had led to the study of some new cathode materials, such as $LiNi_xCo_{1-x}O_2$, $LiFePO_4$ and $LiNi_xCo_yMn_{1-x-y}O_2$.

The optimum electrode material should combine lower cost as well as greater safety and performance compared to $LiCoO_2$. The sample had lower cost for the use of nickel and manganese, which were both abundant in the lithosphere. When it was charged to 4.6 V and then discharged to 2.5 V, it manifested the specific capacity of 200 mAh g^{-1}, which was higher than $LiCoO_2$ without sacrificing circle life. Having been charged to 4.4 V and analyzed by thermogravimetry/differential thermal analysis (TG/DTA), it had much less heat flow and higher onset temperature than $LiCoO_2$.

$LiNi_{1/3}Mn_{1/3}Co_{1/3}O_2$ was first proposed by Ohzuku and Makimura [2]. They initially prepared it by solid state reaction method and re-prepared by mixed hydroxide method [3]. Chowdari and co-workers [4] also prepared it at 1000 °C by mixed hydroxide method and reported that the predominant oxidation states of Ni, Co and Mn in the compound were 2^+, 3^+ and 4^+, respectively. However, a closer inspection of their results reveals some contradictory information on the electrochemical behavior, such as the shape of initial charge curve, reversible capacity and cyclic performance. This strongly implied that the electrochemical characteristics of $LiNi_{1/3}Mn_{1/3}Co_{1/3}O_2$ are prone to be affected by preparation condition. Li et al. studied [5] the influence of preparation method on the structural and electrochemical characteristics of $LiNi_{1/3}Mn_{1/3}Co_{1/3}O_2$ in order to further improve its electrochemical performance, and found that

* Corresponding author. Tel.: +86 10 6275 3288; fax: +86 10 6275 5290.
E-mail address: heping@pku.edu.cn (P. He).

0378-7753/$ – see front matter © 2006 Published by Elsevier B.V.
doi:10.1016/j.jpowsour.2006.01.053

the difference in preparation method resulted in the difference in the color and morphology (shape, particle size and specific surface area) and thereby the difference in the shape of the first charge curve, reversible capacity and the rate capability.

Mixed hydroxide method was a usual method to get the precursor of $LiNi_{1/3}Mn_{1/3}Co_{1/3}O_2$; Lee et al. [6] had done much work on the synthetic optimization of the synthesis of $Mn_{1/3}Ni_{1/3}Co_{1/3}(OH)_2$. But in hydroxide co-precipitation method, Mn^{2+} ion is precipitated as $Mn(OH)_2$ but oxidized gradually to Mn^{3+} (MnOOH) or Mn^{4+} (MnO_2) in aqueous solution. Therefore, preparing the precursor reproductively is very difficult. However, in carbonate homogeneous precipitation method, the oxidation state of Mn is always 2^+ and stable in aqueous solution, thereby very effective for industrial application owing to its high reproducibility. Cho et al. [7] studied the effect of calcination temperature on the character of $LiNi_{1/3}Mn_{1/3}Co_{1/3}O_2$ with $Mn_{1/3}Ni_{1/3}Co_{1/3}CO_3$ as the precursor; we feel the effects of synthetic condition on the precursor should also be studied.

2. Experimental

For preparing transition metal carbonate powders $Mn_{1/3}Ni_{1/3}Co_{1/3}CO_3$, we used $MnSO_4{\cdot}4H_2O$, $NiSO_4{\cdot}6H_2O$, $CoSO_4{\cdot}7H_2O$ and NH_4HCO_3 as the starting materials, all of which were of technical grade and used without further purification. An aqueous solution of $Co_{1/3}Ni_{1/3}Mn_{1/3}SO_4$ with a concentration of 0.5 mol m^{-3} was pumped into a continuously stirred tank reactor (CSTR, volume 1 l). At the same time, NH_4HCO_3 solution of 2.0 mol dm^{-3} was also fed into the reactor. The reaction temperature and feed rate of the reactants to the reactor were controlled carefully. After vigorous stirring at 75–90 °C for 12 h, the homogenously precipitated carbonate powder $Mn_{1/3}Ni_{1/3}Co_{1/3}CO_3$, hereafter referred as a precursor, was filtered off and dried without washing at 110 °C for 10 h. Then, EDTA titration was applied to decide exact amount of transition metal ions which were mixed with lithium salt in the pre-heated powder. To synthesize $LiNi_{1/3}Mn_{1/3}Co_{1/3}O_2$ material, a more than stoichiometric amount of lithium hydroxide was mixed with the pre-heated powders and calcined at 500 and 1000 °C, respectively, in air.

Powder X-ray diffraction (XRD) employing Cu Kα radiation was used to identify the crystalline phase of the prepared powders by means of an X-ray diffractometer (MultFlex, Rigacu, Japan). The shape and size of the as-prepared samples were observed by scanning electronic microscope (SEM, JSM-5600LV, JEOL, Japan). The concentrations of lithium and cobalt, nickel, manganese, etc., in the resulting materials were analyzed using an inductively coupled plasma spectrometer (ICP, Optima 4300DV, PE Ltd.). Charge–discharge tests were performed with coin type cell (CR2032) with applying a current density of 20 mA g^{-1} at 25 °C. Composite positive electrodes were prepared by thoroughly mixing the active material (80 wt%) with carbon black (5 wt%), acetylene black (5 wt%) and polyvinylidene fluoride (10 wt%) in *N*-methyl-pyrrolidinone and extruding onto aluminium foils. Electrodes, with loading between 8 and 10 mg active material cm^{-2}, were dried for 24 h at 110 °C in electric oven under vacuum. CR2032 simulated half cells were then assembled in a helium filled dry box (<1 ppm O_2/H_2O) using foils of Li metal as counter electrodes and Celgard 3401 saturated with a 1 M $LiPF_6$ (electrolyte) in ethylene carbonate/diethyl carbonate (1:1, v/v). Several simulated cells containing each sample were assembled and tested, to ensure reproducibility.

3. Results and discussion

3.1. The choice of the reaction temperature of precipitation

During the precipitation process, the crystals endured two steps: the formation of crystal nuclei and their growing up which includes each single crystal nucleus development and the agglomeration of some nuclei. The well formed and high-density particles can be prepared with the decrease of temperature for the lower nucleus concentration and lower growing rate [7]. For the reason of complexation of cobalt and nickel by ammonia, little precipitate can emerge when the temperature is low, which decreased the product capacity. When the feed rate is 20 ml min^{-1}, and molar ratio of the metal to ammonia is 2.5, Table 1 shows the concentrations of cobalt, nickel and manganese in the solution after reaction at different temperatures. While the reaction temperature increases, the concentrations of cobalt, nickel and manganese decrease promptly. Considering the importance of tap density of the final sample and product capacity, the reasonable reaction temperature should be chosen as 80 °C.

3.2. The effect of feed rate

Feed rate is an important factor that can affect the possibility of industrialization. Lower feed rate decreases the production capacity, then increases the production cost. And lower feed rate decreases the nucleation speed and causes fewer nuclei to be formed. Although the speed of nuclei growth was also lowered, it was still higher than the nucleation speed. For the

Table 1
The concentration of cobalt, nickel and manganese in the solution and the tap density of $LiNi_{1/3}Mn_{1/3}Co_{1/3}O_2$ at different temperatures

Temperature (°C)	Cobalt (mg ml^{-1})	Nickel (mg ml^{-1})	Manganese (mg ml^{-1})	Tap density of $LiNi_{1/3}Mn_{1/3}Co_{1/3}O_2$ (g cm^{-3})
60	8.41	13.52	0.47	2.32
70	2.19	5.28	0.12	2.21
80	0.93	2.06	0.05	2.19
90	0.27	0.84	0.02	1.77

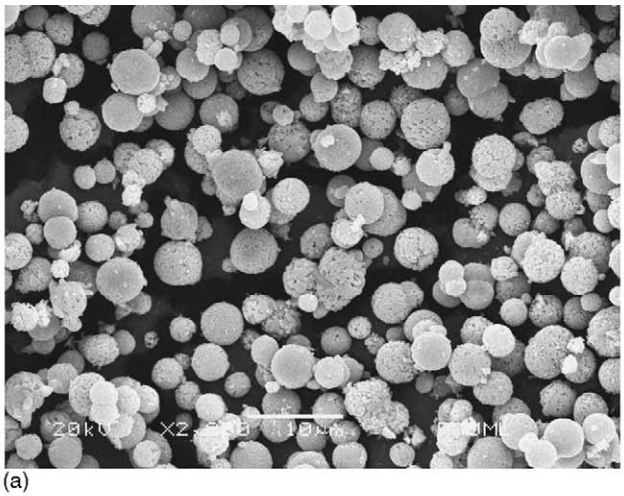

(a)

(b)

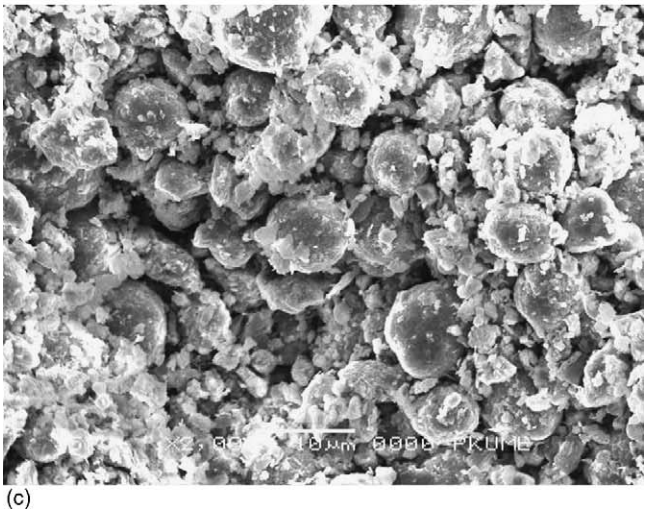

(c)

Fig. 1. SEM images of the precursor at different feed rates of the metal solution: (a) 10 ml min^{-1}, (b) 20 ml min^{-1} and (c) 30 ml min^{-1}.

reason of microcrystal agglomeration, larger crystal could be obtained. When improving feed rate, high concentration of reactants improves the nucleation rate, leading to more nuclei and loose crystal emerges. Fig. 1 shows the particles obtained at 80 °C and molar rate of 2.5 with different feed rates.

Considering the precursor morphology and the production cost, the suitable feed rate should be chosen as 20 ml min^{-1} during the experiment.

3.3. The effect of the molar ratio of the total metal ion to the ammonia bicarbonate

As we know, the complexation of metal ion with ammonia will be weakened by the high concentration of carbonate. Much more precipitate should be obtained by increasing the concentration of ammonia bicarbonate, which means higher molar ratio of the metal ion to the ammonia bicarbonate should be chosen. But with the concentration of the ammonia bicarbonate increasing, the morphology of the precursor turns loose, the tap density decreases promptly, which is shown in Fig. 2 with the feed rate of 20 ml min^{-1} and 80 °C.

In Table 2, the concentrations of metal ions in the solution after the precipitation and the final sample tap density are compared at different molar ratios of the total metal ion to the ammonia bicarbonate. Although the tap density decreases all through the molar ratio increasing, the concentration of metal ion increases after the molar ratio is higher than 3, for the higher ammonia concentration can dissolve the precipitate then.

3.4. Preparation of $LiNi_{1/3}Mn_{1/3}Co_{1/3}O_2$ by high temperature calcination

Fig. 3 shows SEM of the product using the precursor obtained at the optimum condition, which exhibited the suitable condition for the scale-up. The prepared metal oxide was calcined with appropriate amount of Li_2CO_3 at 500 and 1000 °C for 12 h in air, respectively. A little amount of excess lithium (Li/Co = 1.05) was incorporated to compensate for the evaporation of lithium during high temperature calcination, resulting in stoichiometric composition in the final products. The synthesized powders had the typical XRD patterns as seen in Fig. 4. The lattice parameters obtained by least-squares fitting of the (h k l) and 2θ values for the compound are: a = 2.861 Å and c = 14.240 Å and match well with the values observed by Ohzuku and Makimura (a = 2.867 Å and c = 14.246 Å) [2]. The clearly split (0 0 6, 0 1 2) and (0 1 8, 1 1 0) pairs in the XRD pattern and the c/a ratio (4.977) well above that required for distortion of oxygen lattice reveal that the layered structure is formed. The integrated intensity ratio of the (0 0 3) to (1 0 4) lines in the XRD patterns was shown to be a measure of the cation mixing and a value of 1.41 is an indication of little undesirable cation mixing [8]. So-prepared product composition was confirmed by ICP analysis (Table 3). Although the samples of technical grade were used as the reactant, and little water was used to wash the precursor, impurity content was still tolerable. When suitable reaction condition is chosen, the same molar ratio of nickel, cobalt and manganese can be obtained.

In order to observe cycling stability at higher voltage, the upper cut-off voltage was charged to 4.2, 4.35 and 4.5 V. The discharge capacities increase gradually by raising the upper cut-off voltage limit. Fig. 5 shows the first charge–discharge profile of different cut-off voltages. In voltage range of 2.8–4.2, 2.8–4.35 and 2.8–4.5 V, the capacities of $LiNi_{1/3}Mn_{1/3}Co_{1/3}O_2$ electrode

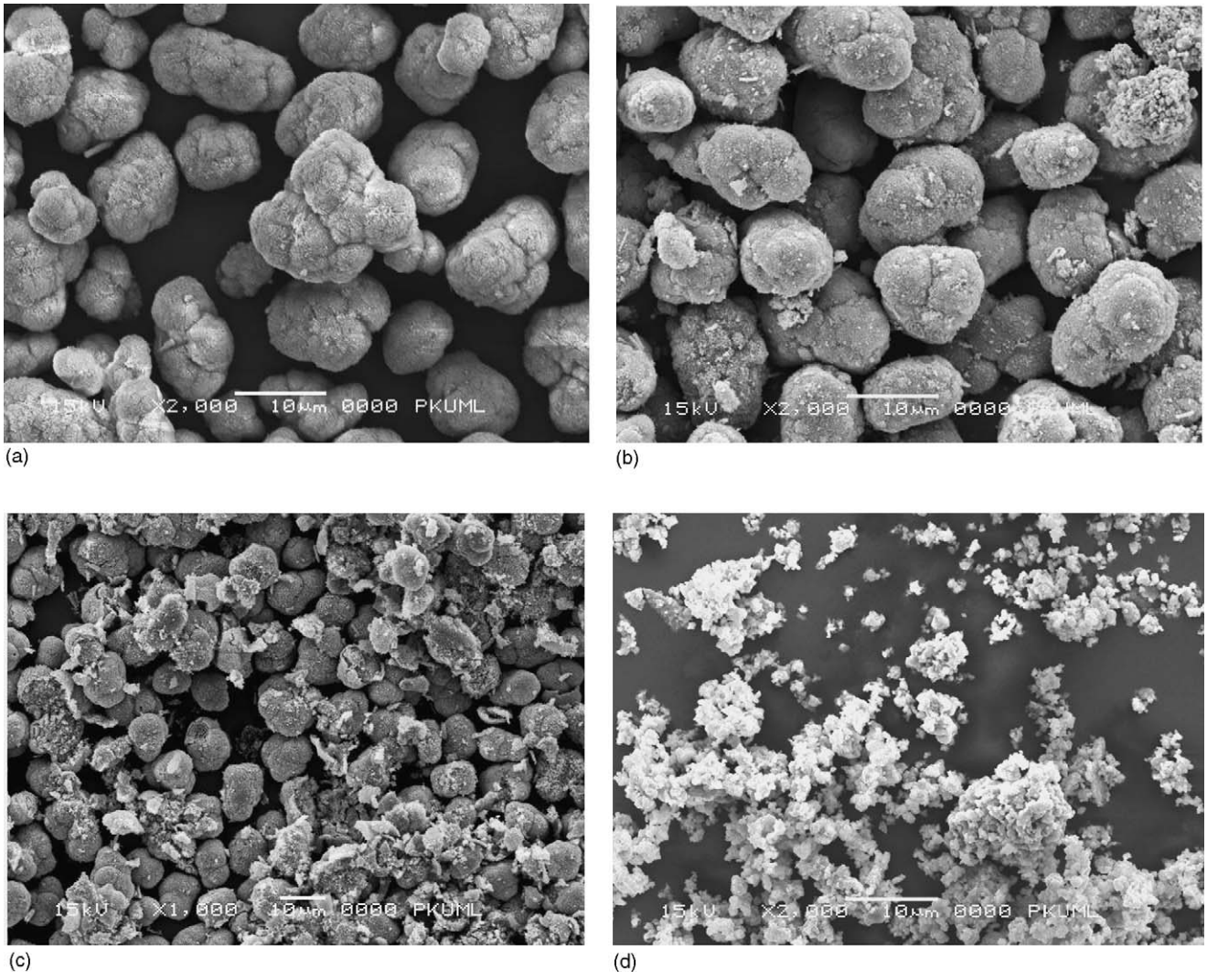

Fig. 2. SEM images of the precursor with different molar ratios of the metal ion to ammonia bicarbonate: (a) 1.5, (b) 2.0, (c) 3.0 and (d) 3.5.

Table 2
The concentration of cobalt, nickel and manganese in the solution and the tap density of $LiNi_{1/3}Mn_{1/3}Co_{1/3}O_2$ at different molar ratios of the metal ion to the ammonia bicarbonate

Molar ratio of M/A	Cobalt (mg ml^{-1})	Nickel (mg ml^{-1})	Manganese (mg ml^{-1})	Tap density of $LiNi_{1/3}Mn_{1/3}Co_{1/3}O_2$ (g cm^{-3})
1.5	6.32	11.17	0.38	2.27
2	3.09	4.71	0.26	2.24
2.5	0.88	1.14	0.12	2.19
3	0.61	0.92	0.03	1.69
3.5	0.91	1.25	0.03	1.48

are 159, 168 and 179 mAh g^{-1}, respectively, with good cyclability as shown in Fig. 6. In fact, it was reported that the occurrence of Co dissolution at higher voltage (>4.3 V) has a very detrimental effect on high voltage operation of $LiCoO_2$. The stable cyclability even at higher voltage limit also suggests that metal dissolution could be greatly suppressed in $LiNi_{1/3}Mn_{1/3}Co_{1/3}O_2$, which needs to be further considered in the future. From the SEM of spherical $LiNi_{1/3}Mn_{1/3}Co_{1/3}O_2$ (Fig. 3), we can learn that its shape did not appear as a single particle like what is in the market. The surface of the powder was an aggregate of many small particles. Each large particle was composed of such small ~1 μm particles, which maybe the excuse for the good electric character because of the easier insertion and desertion of lithium. It is well known that the specific surface area is an important factor to stabilize the performance of lithium secondary batteries.

Table 3
Element content of the precursor and $LiNi_{1/3}Mn_{1/3}Co_{1/3}O_2$

	Li	Ni	Co	Mn	Ca	Fe	Na
Precursor		24.21	24.73	23.46	0.018	0.013	0.003
Product	7.52	19.95	20.59	19.08	0.012	0.011	0.003

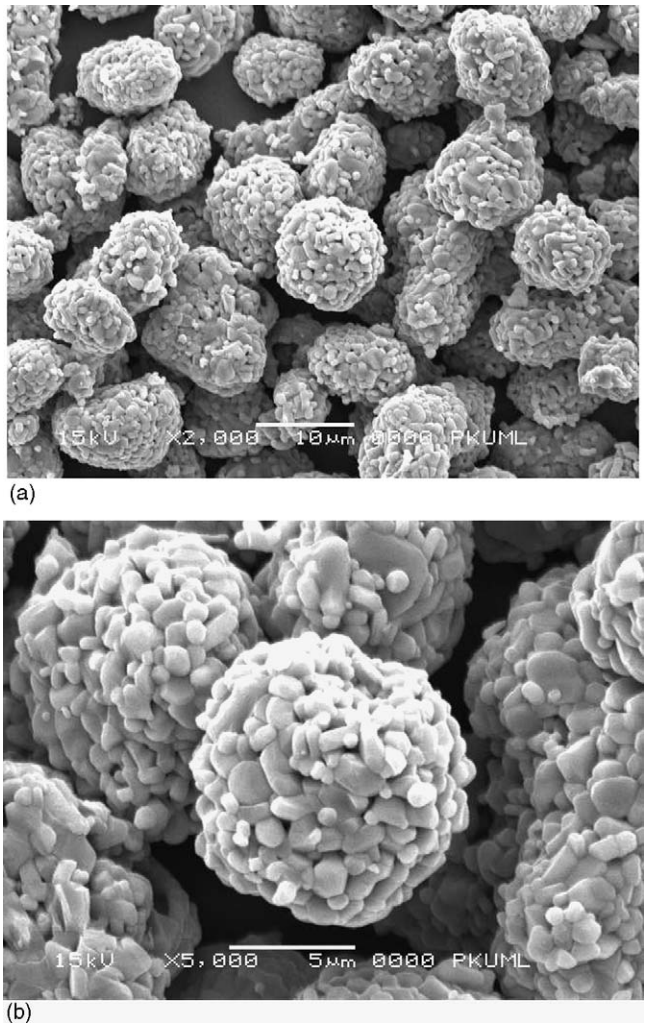

Fig. 3. SEM images of spherical sample of (a) low and (b) high magnification calcined at 500 and 1000 °C for 12 h in air.

When lithium and the pre-calcined precursors were calcined in the furnace, the small particles were agglomerated into large micro-sized particles by continuous calcination. Although there was a high possibility that a significantly increased surface area of $LiNi_{1/3}Mn_{1/3}Co_{1/3}O_2$ would result in the collapse of the structure due to an excess reaction between the very small particles

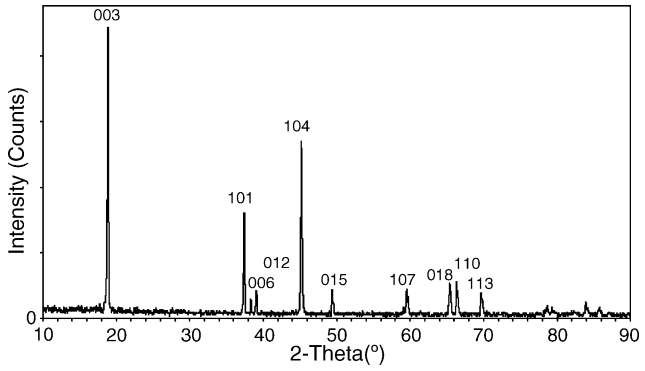

Fig. 4. Powder XRD pattern of the prepared $LiNi_{1/3}Mn_{1/3}Co_{1/3}O_2$.

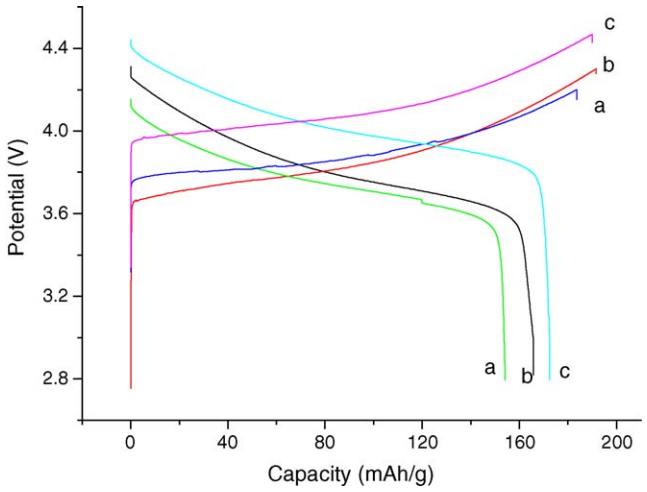

Fig. 5. First charge–discharge profile for $LiNi_{1/3}Mn_{1/3}Co_{1/3}O_2$ at different cut-off voltages: (a) 2.8–4.2 V, (b) 2.8–4.35 V and (c) 2.8–4.5 V.

and electrolyte, well optimized synthetic conditions using the carbonate precipitation process could maintain the most favorable powder properties of $LiNi_{1/3}Mn_{1/3}Co_{1/3}O_2$, which existed in the form of agglomeration. Actually, even though the spherical crystal had four to five times smaller primary particle size, its surface area was nearly the same as that of single particle. Therefore, we found that the average particle size and surface area of the resulting powder could be controlled during the synthesis and calcination processes.

For practical applications, tap density of active material is also important to decide the capacity of battery. Because the inner space of battery is limited, if the tap density is high, the higher volumetric capacity can be obtained, though the same gravimetric capacity remains. As a result, higher tap density will lead to higher volumetric capacity in practical cells. Therefore, it is concluded that the preparation of homogeneous spherical precursor is a critical factor for synthesis of high quality materials.

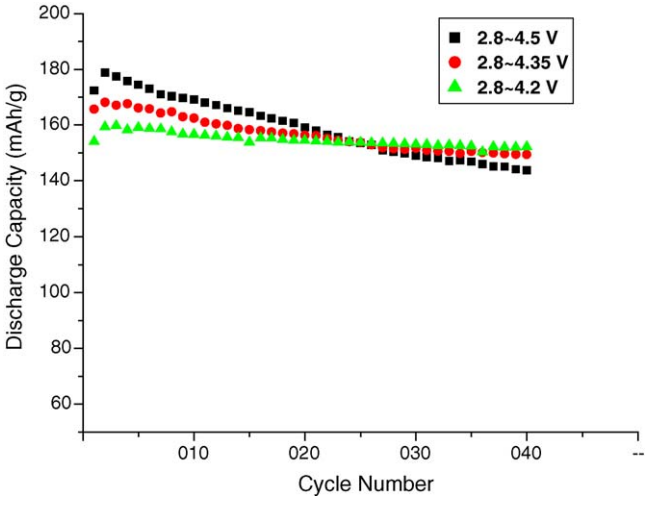

Fig. 6. Electrochemical performance of final sample with different cut-off voltages.

4. Conclusion

Uniform-phase precipitation method has been employed to synthesize the spherical-shaped $Ni_{1/3}Mn_{1/3}Co_{1/3}CO_3$ by carefully controlling the reaction temperature, feed rate and molar rate of metal ion to ammonia bicarbonate. The optimum condition is 80 °C, 20 ml min^{-1} feed rate and 2.5 molar rate of M/A to get dense precursor. After calcination with lithium hydroxide, $LiNi_{1/3}Mn_{1/3}Co_{1/3}O_2$ could be obtained with the tap density as 2.19 g cm^{-3}. In the voltage range of 2.8–4.2, 2.8–4.35 and 2.8–4.5 V, the capacities of $LiNi_{1/3}Mn_{1/3}Co_{1/3}O_2$ electrode are 159, 168 and 179 mAh g^{-1}, respectively.

Acknowledgements

The authors would like to thank Prof. Toshiyuki Momma of Department of Applied Chemistry, Waseda University, Prof. Masataka Wakihara and Dr. Masanobu Nakayama of Tokyo Institute of Technology, and Prof. Xiangyun Wang of Peking University for their helpful discussion.

References

[1] P. He, H. Wang, L. Qi, T. Osaka, J. Power Sources, in press.
[2] T. Ohzuku, Y. Makimura, Chem. Lett. 1 (2001) 642.
[3] N. Yabuuchi, T. Ohzuku, J. Power Sources 119 (2003) 171.
[4] K.M. Shaju, G.V. Subba Rao, B.V.R. Chowdari, Electrochim. Acta 48 (2002) 145.
[5] D.-C. Li, T. Muta, L.-Q. Zhang, M. Yoshio, H. Noguchi, J. Power Sources 132 (2004) 150–155.
[6] M.-H. Lee, Y.-J. Kang, S.-T. Myung, Y.-K. Sun, Electrochim. Acta 50 (2004) 939–948.
[7] T.H. Cho, S.M. Park, M. Yoshio, T. Hirai, Y. Hideshima, J. Power Sources 142 (2005) 306–312.
[8] T. Ohzuku, A. Ueda, M. Nagayama, Y. Iwakoshi, H. Komori, Electrochim. Acta 38 (1993) 1159.